Cardiovascular Research (2011) **89**, 680–688
doi:10.1093/cvr/cvq340

Molecular MRI of murine atherosclerotic plaque targeting NGAL: a protein associated with unstable human plaque characteristics

Bernard C. te Boekhorst[1,2*†], Sandra M. Bovens[1,2†], Willem E. Hellings[3], Petra H. van der Kraak[4], Kees W. van de Kolk[1], Aryan Vink[4], Frans L. Moll[3], Matthijs F. van Oosterhout[5], Jean P. de Vries[6], Pieter A. Doevendans[1,2], Marie-José Goumans[7], Dominique P. de Kleijn[1,2], Cees J. van Echteld[1], Gerard Pasterkamp[1], and Joost P. Sluijter[1,2]

[1]Experimental Cardiology Laboratory, Department of Cardiology, University Medical Center Utrecht, Heidelberglaan 100, Room G02.523, 3584 CX Utrecht, The Netherlands; [2]Interuniversity Cardiology Institute of the Netherlands (ICIN), The Netherlands; [3]Department of Vascular Surgery, University Medical Center, Utrecht, The Netherlands; [4]Department of Pathology, University Medical Center, Utrecht, The Netherlands; [5]Department of Pathology, St Antonius Hospital, Nieuwegein, The Netherlands; [6]Department of Vascular Surgery, St Antonius Hospital, Nieuwegein, The Netherlands; and [7]Department of Molecular Cell Biology, Leiden University Medical Center, Leiden, The Netherlands

Received 15 October 2009; revised 18 October 2010; accepted 25 October 2010; online publish-ahead-of-print 28 October 2010

Time for primary review: 27 days

Aims Neutrophil gelatinase-associated lipocalin (NGAL) is an effector molecule of the innate immune system. One of its actions is the prolongation of matrix metalloproteinase-9 (MMP-9) activity by the formation of a degradation-resistant NGAL/MMP-9 complex. We studied NGAL in human atherosclerotic lesions and we examined whether NGAL could act as a target for molecular imaging of atherosclerotic plaques.

Methods and results Increased levels of NGAL and the NGAL/MMP-9 complex were associated with high lipid content, high number of macrophages, high interleukin-6 (IL-6) and IL-8 levels, and low smooth muscle cell content in human atherosclerotic lesions obtained during carotid endarterectomy ($n = 122$). Moreover, plaque levels of NGAL tended to be higher when intra-plaque haemorrhage (IPH) or luminal thrombus was present ($n = 77$) than without the presence of IPH or thrombus ($n = 30$). MMP-9 and -8 activities were strongly related to NGAL levels. The enhancement on magnetic resonance (MR) images of the abdominal aorta of $ApoE^{-/-}/eNOS^{-/-}$ mice was observed at 72 h after injection of NGAL/24p3-targeted micelles. The specificity of these results was validated by histology, and co-localization of micelles, macrophages, and NGAL/24p3 was observed.

Conclusion NGAL is highly expressed in atheromatous human plaques and associated with increased MMP-9 activity. NGAL can be detected in murine atherosclerotic arteries using targeted high-resolution MR imaging. Therefore, we conclude that NGAL might serve as a novel imaging target for the detection of high-risk plaques.

Keywords Atherosclerosis • Matrix metalloproteinases • Macrophages • Contrast agents • Molecular MRI

1. Introduction

In vivo imaging of proteins which are associated with atherosclerotic disease progression and plaque destabilization is a major challenge. Magnetic resonance imaging (MRI) provides both a high anatomical detail and the option of molecular MRI of plaque proteins. Molecular MRI, using gadolinium (Gd)-loaded nanoparticles, of macrophage and cholesterol metabolism-related targets in early to intermediate plaques has revealed promising results.[1–5] Micelles are lipid-based nanoparticles, in the nanometre range, and may be coated with poly-ethylene-glycol (PEG) to extend plasma half-lives.[6] The possibility to bind antibodies to PEG and to incorporate Gd and fluorescent probes makes these particles very suitable for targeted MRI of the high-risk atherosclerotic plaque.

* Corresponding author. Tel: +31 88 7557155; fax: +31 30 2522693, Email: b.t.boekhorst@tue.nl

† These authors contributed equally to this work.

Neutrophil gelatinase-associated lipocalin (NGAL) is a 25 kDa glycoprotein which was first discovered in human neutrophils.[7,8] NGAL is an effector molecule of the innate immune system through the inhibition of bacterial iron uptake by binding bacterial siderophores.[9] Moreover, it mediates inflammatory activity through binding to formyl-methionyl-leucyl-phenylalanine (fMLP; a chemotactic peptide), leukotriene B4, and platelet-activating factor.[10–12] The production of NGAL is induced via nuclear factor kappa B, and high levels are found in inflammatory conditions.[11,13] NGAL is able to form a stable, biologically active complex with matrix metalloproteinase-9 (MMP-9), preventing its degradation and thereby prolonging MMP-9 activity.[14] In addition, NGAL is involved in the allosteric activation of MMP-8 and -9.[15]

MMPs are key players in atherosclerotic disease. They are capable of degrading a broad spectrum of extracellular matrix components and held responsible for vascular remodelling and breakdown of the fibrous cap of atherosclerotic lesions.[16] Especially, MMP-9 is implicated to play a crucial role in atherosclerotic plaque destabilization, both in human studies and experimental models.[17–21] The mouse analogue of NGAL, called 24p3 (SIP24, lipocalin-2, uterocalin), was present in murine atherosclerotic lesions, as demonstrated by Hemdahl *et al.*[22] Considering the function of NGAL in the innate immune system and its effect on MMP-9 activity, NGAL might play an important role in atherosclerotic plaque destabilization.

We studied whether NGAL is associated with histological characteristics of high-risk human atherosclerotic lesions and whether MRI of micelles, targeting NGAL, is feasible in the ApoE$^{-/-}$/eNOS$^{-/-}$ mouse model[23] and thereby could serve as a novel target to visualize high-risk atherosclerotic lesions.

2. Methods

2.1 Human carotid atherosclerotic artery specimens

Carotid plaques were obtained from a consecutive series of patients undergoing carotid endarterectomy (CEA; $n = 122$), participating in the Athero-Express biobank.[24] This ongoing biobank is running in two Dutch hospitals: The University Medical Center Utrecht and the St Antonius Hospital Nieuwegein. These patients all suffered from high-grade (>70%) carotid stenosis. Indications for CEA were based on recommendations from the NASCET, ECST, ACAS, and ACST trials.[25–28] The investigations conformed to the principles outlined in the Declaration of Helsinki. The study was approved by the institutional review boards of both participating hospitals and all patients provided written informed consent.

2.2 Carotid plaque characterization

The CEA specimens were divided in segments of 5 mm thickness along the longitudinal axis of the vessel.

The segment with greatest plaque burden was embedded in paraffin for further histological characterization. Staining for macrophages, endothelial cells, smooth muscle cells (SMCs), and NGAL was performed. Semi-quantitative analysis of plaque for macrophages, SMCs, collagen, lipid content, calcifications, and overall phenotype followed. Additionally, the presence of intra-plaque haemorrhage (IPH) or luminal thrombus was scored by checking for (remnants of) erythrocytes and fibrin strands on HE stainings.

The directly adjacent segment was used for protein extraction. Interleukin-6 (IL-6), IL-8, MMP-2, -8, and -9 activities in the protein extracts were measured with an activity assay. See Supplementary material online for further details.

2.3 Detection of NGAL in carotid plaques

For immunohistochemical detection of the NGAL/MMP-9 complex in carotid plaques, see Supplementary material online.

NGAL/MMP-9 complex activity was determined using gelatin zymography ($n = 122$) (see Supplementary material online).

Additionally, NGAL concentration in protein extracts of the tissue specimens was measured with an NGAL enzyme-linked immunosorbent assay (ELISA) kit ($n = 107$), according to the manufacturer's protocol (Antibodyshop, Gentofte, Denmark). This assay has no cross-reactivity with NGAL/MMP-9 complexes. The measurements were standardized for total protein concentration of the protein extracts.

2.4 Release of NGAL and NGAL/MMP-9 complex from carotid plaques

To assess the release of NGAL or NGAL/MMP-9 complexes from plaques into the systemic circulation, we applied a novel model comparable to the system applied by Maier *et al.*[29] A blood sample obtained at the site of the plaque was compared with a peripheral blood sample for the concentration of NGAL and NGAL/MMP-9 complex in nine consecutive patients undergoing CEA. The difference in concentration between the local and peripheral obtained samples is a measure of secretion of the protein by the plaque. During CEA, the blood sample at the plaque site ('plaque-related blood') was drawn directly from the already exposed common carotid artery. This was done after the blood had been halted for 2 min at the plaque site during test-clamping, which is routinely performed in our hospital before incision of the carotid artery. At exactly the same time, a peripheral blood sample was drawn from the indwelling arterial line in the radial artery. NGAL was measured by ELISA as described above. Levels of the NGAL/MMP-9 complex were determined by ELISA (R&D Systems, Minneapolis, MN, USA).

2.5 Murine aortic atherosclerotic specimens

2.5.1 Animals

Animal experiments conformed to the Guide for the Care and Use of Laboratory Animals published by the US National Institutes of Health (NIH Publication No. 85-23, revised 1996) and they were approved by the animal experimental committee of the Utrecht University. Old (between 9 and 12 months) male ApoE/eNOS double-knockout mice (generated in our lab by crossing the offspring of ApoE$^{-/-}$ and eNOS$^{-/-}$ mice, genotype confirmed by PCR) were fed a western-type diet (Harlan) for 12 weeks. In Group A1 ($n = 6$), mice were injected with NGAL-targeted micelles and imaged at baseline and $t = 24$ h. In Group A2 ($n = 8$), mice were injected with NGAL-targeted micelles and imaged at baseline, $t =$ 24, and 72 h. In Group B1 ($n = 4$), mice were injected with isotype-conjugated micelles (control) and imaged at baseline and $t = 24$ h. In Group B2 ($n = 6$), mice were injected with isotype-conjugated micelles (control) and imaged at baseline, $t = 24$, and 72 h.

2.5.2 Validation of the unstable plaque mouse model

The histology from abdominal aortic plaques in ApoE/eNOS double-knockout mice was compared with the histology from a well-accepted unstable plaque mouse model in the literature[30] (brachiocephalic artery plaque of an apoE knockout mouse on an atherogenic diet).

2.5.3 Micelles

A mixture of the appropriate amounts of lipids (DSPE-PEG2000 (43 M%), Gd-DTPA-bisstearylamide (50 M%), Liss-Rhod-PE (5 M%), and Mal-PEG2000-DSPE (2 M%) (all purchased from Avanti Polar Lipids Inc., Alabaster, AL, USA), dissolved in chloroform, was dried by rotary evaporation at 55°C. The lipid film was subsequently hydrated in 1 mL phosphate-buffered

saline (PBS), yielding a total lipid concentration of 3 mM. Rat anti-mouse 24p3 antibodies (3 mg/mL) (MAB1857, R&D systems) and rat IgG isotype antibodies (Invitrogen, Carlsbad, CA, USA) were conjugated via SATA modification as described previously.[31] The modified antibody was added to the micelles and incubated overnight at 4°C. According to size-exclusion chromatography, >95% of antibodies were bound to mal-PEG (data not shown). Given that the molar antibody to the lipid ratio was 0.7:100 and the percentage of mal-PEG was 2%, ~35% of mal-PEG should be occupied by an antibody. Assuming that these micelles are composed of ~100 lipid monomers, nearly all micelles were occupied by antibodies.

Rat isotype and 24p3 antibody-conjugated micelles had a size of ~23 nm determined by dynamic light scattering (data not shown).

2.5.4 Animal preparation and anesthesia

Mice were imaged in a vertical 9.4 T, 89 mm bore size magnet equipped with a 1500 mT/m gradient set and connected to an Avance 400 MR system (Bruker BioSpin, Germany) in a quadrature-driven birdcage coil with an inner diameter of 3 cm. ParaVision 4.0 software was used for MR acquisition and reconstruction.

Mice were anaesthetized with 5 vol% isoflurane in a 2:1 mixture of air (0.3 L/min) and oxygen (0.15 L/min) and maintained with 1.5–2.5 vol% isoflurane to keep the respiratory rate stable. An intravenous catheter was inserted into the tail vein. The cardiac and respiratory motions were monitored using a respiratory pad linked to an ECG/respiratory unit.

2.6 Baseline and follow-up MRI procedure

After scout imaging was performed, 20 contiguous axial slices were planned from 4 mm below the right renal artery branch up to 5 mm above this branch. Inversion recovery-fast spin echo images and anatomic reference images for lymph nodes and peri-aortic blood vessels were made.

See Supplementary material online for further details.

2.7 Contrast injection, harvesting, and preparation of aortas

After the baseline MRI procedure, 200 μL of contrast agent (3 mM lipid 24p3-targeted or isotype-conjugated micelles) was injected via an intravenous catheter, the catheter was removed, and the animal recovered from anaesthesia until the next MRI procedure. After the last MRI procedure, anaesthesia was continued with a mixture of medetomidine (6%)/ketamine (5%) (0.1 mL/10 g). The imaged parts of the aortas were harvested after perfusion with nitroglycerin/PBS (1:10), perfusion-fixated with formaldehyde 4%/PBS (1:10), and embedded in paraffin or perfused with OCT compound/PBS (1:10) and embedded in OCT compound and stored at −20°C.

2.8 Histology of murine atherosclerotic specimens

From 4 mm caudal to 5 mm cranial of the right renal artery branch, sections were made at every 0.5 mm. Staining for lipids, macrophages, 24p3, and micelles was performed. See Supplementary material online for further details. In the case of validation of the plaque mouse model, carotid arteries and aortas were stained for SMCs (buried fibrous caps[30]), iron (IPH[32]), and NGAL.

2.9 MRI and histological review

MRI data were reviewed independently (B.C.B. and S.M.B), and regions of interest representing the pre-vertebral (pv) muscle and plaque were drawn on pre- and post-injection images. The normalized enhancement ratio (NER) was derived from the signal intensity (SI) of plaque and pv muscle (SI_{plaque} and $SI_{pv\ muscle}$) using the formula:

$$\frac{(SI_{plaque}/SI_{pv\ muscle(post-injection)})}{(SI_{plaque}/SI_{pv\ muscle(pre-injection)})}$$

2.10 Data analysis

All measurements are presented as mean ± SEM. Associations between carotid plaque composition parameters and NGAL or NGAL/MMP-9 complex levels in the plaque were tested by the Mann–Whitney *U* test or Spearman's non-parametric correlation where appropriate. Wilcoxon's

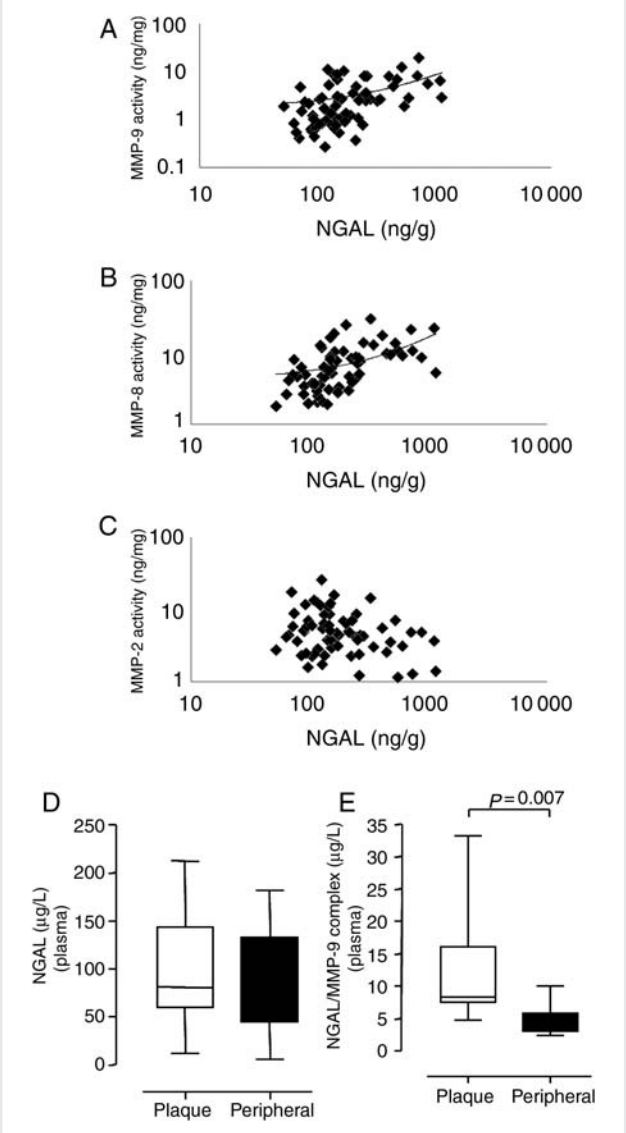

Figure 1 Association between NGAL and MMP activity; blood and plaque levels of NGAL and NGAL/MMP-9 in humans. (*A*) Association between plaque NGAL concentration and plaque MMP-9 activity (ELISA) ($R = 0.528$; $P < 0.001$). (*B*) Association between plaque NGAL concentration and plaque MMP-8 activity (ELISA) ($R = 0.654$; $P < 0.001$). (*C*) Association between plaque NGAL concentration and plaque MMP-2 activity (ELISA) (P = n.s.). (*D*) NGAL concentrations: local plaque-related blood vs. peripheral blood ($n = 9$; $P = 0.06$). (*E*) NGAL/MMP-9 concentrations: local plaque-related blood vs. peripheral blood ($n = 9$; $P = 0.007$).

signed-rank test was used to test significance for the carotid plaque secretion experiments. To adjust the relation between MMP-9 and NGAL for the presence of macrophages, a linear regression model was constructed in which 'NGAL' and 'number of plaque macrophages' were entered as determinants and MMP-9 as the predicted variable. Differences in NER between mouse groups were tested with the independent sample *t*-tests. $P \leq 0.05$ were considered statistically significant.

3. Results

3.1 Association between NGAL and MMP levels in atherosclerotic carotid plaques

In atherosclerotic carotid plaques, a strong positive correlation was observed between total NGAL content and total MMP-9 (*Figure 1A*; $R = 0.528$; $P < 0.001$) and MMP-8 activity (*Figure 1B*; $R = 0.654$; $P < 0.001$) as determined by the activity assay. No association with MMP-2 activity could be observed (*Figure 1C*). MMP-9 activity correlated with NGAL/MMP-9 levels in the plaques (see Supplementary material online, *Figure S1A*) and NGAL appears to preserve MMP-9 activity (see Supplementary material online, *Figure S2*).

We investigated whether the strength of the association between NGAL and MMP-9 levels might be influenced by the number of macrophages in the plaque. Therefore, we rectified the relation between NGAL and MMP-9 levels for the extent of macrophage infiltration and put these variables in a linear regression model. This model demonstrated that NGAL levels were associated with MMP-9 levels, independently on the presence of macrophages ($\beta = 0.43$; $P < 0.001$).

3.2 Interaction of NGAL and MMP-9 in atherosclerotic carotid plaques

Gelatinolytic activity of NGAL/MMP-9 complexes (see Supplementary material online, *Figure S1B*) was detected at 125 kDa (NGAL/MMP-9) and 150 kDa (NGAL-dimer/MMP-9) as previously described by Yan *et al.*[14] This was confirmed via western blotting: specific NGAL bands were detected at 125 and 150 kDa, corresponding to the two bands observed in zymography (see Supplementary material online, *Figure S1B*). In addition, free NGAL was detected by western blotting at 25 kDa (monomer) and 50 kDa (dimer; data not shown). The NGAL/MMP-9 complexes could be reconstructed *in vitro* by incubation of MMP-9 and NGAL recombinants (see Supplementary material online, *Figure S2*). Gelatinolytic activity of the NGAL/MMP-9 complex was significantly higher in carotid artery plaques compared with the control mammary arteries (see Supplementary material online, *Figure S1C*). Moreover, as can be appreciated in Supplementary material online, *Figure S1C*, an important part of total gelatinolytic activity in the plaques was attributable to the NGAL/MMP-9 complexes (6.75 AU) compared with free MMP-9 (15.3 AU), which

Table 1 Relation between plaque characterization and expression of NGAL

Plaque characteristics	NGAL/MMP-9 gelatinolytic activity (AU)	*P*-value	NGAL (ng/mg)	*P*-value
n	122		107	
Overall				
Fibrous	4.6 ± 1.0		158 ± 20	
Fibr-Ath	7.0 ± 0.8		314 ± 51	0.05
Atheromatous	7.4 ± 0.9	0.043	255 ± 30	0.004
MO				
Minor	6.2 ± 0.8	0.1	247 ± 44	0.9
Heavy	7.2 ± 0.7		195 ± 30	
SMC				
Minor	7.6 ± 0.9	0.03	288 ± 46	0.1
Heavy	6.1 ± 0.6		209 ± 49	
MO/SMC				
SMC dominant	6.0 ± 0.7	0.03	280 ± 36	0.8
MO dominant	8.4 ± 0.3		245 ± 50	
Collagen				
Minor	7.6 ± 1.0	0.08	262 ± 37	0.3
Heavy	6.3 ± 0.6		239 ± 56	
Calcifications				
Minor	7.0 ± 0.7	0.6	379 ± 72	0.1
Heavy	6.5 ± 0.8		180 ± 22	
IL-6				
Low[a]	5.8 ± 0.8	0.1*	207 ± 27	0.02*
High[b]	6.9 ± 0.8		304 ± 39	
IL-8				
Low[a]	4.5 ± 0.6	<0.001*	147 ± 11	<0.001*
High[b]	8.6 ± 0.8		384 ± 45	

All values are presented as mean ± standard error of the mean. Fibr-Ath, fibro-atheromatous; MO, macrophage infiltration; SMC, smooth muscle cell infiltration; IL, interleukin.
*Spearman's correlation: [a]low: <median; [b]high: ≥median. Significance level: $P \leq 0.05$.

was confirmed by quantification of the NGAL/MMP-9 complex levels via ELISA in a subset of samples (0.60 vs. 2.51 ng/g, respectively). Gelatinolytic activity of the NGAL/MMP-9 complex was strongly related to NGAL concentration ($R = 0.310$; $P = 0.001$) and MMP-9 activity (see Supplementary material online, *Figure S1A*; $R = 0.315$; $P = 0.005$), whereas NGAL/MMP-9 gelatinolytic activity was not associated with MMP-8 or -2 activity levels (data not shown).

3.3 Association between NGAL and unstable plaque phenotype

NGAL levels were higher in plaques with an unstable phenotype (*Table 1*). Fibro-atheromatous plaques had higher NGAL content and atheromatous plaques had higher NGAL/MMP-9 activity and NGAL content when compared with fibrous plaques. Plaques with more macrophages demonstrated higher NGAL/MMP-9 activity and plaques with high levels of pro-inflammatory cytokines IL-6 and IL-8 had higher NGAL content and demonstrated higher NGAL/MMP-9 activity than stable plaques that are fibrous and have higher SMC content. Further, plaque NGAL/MMP-9 activity was higher with minor staining for SMCs when compared with heavy staining ($P = 0.03$). Additionally, plaque levels of NGAL tended to be higher when IPH or luminal thrombus was present ($n = 77$) than without the presence of IPH or thrombus ($n = 30$) ($P = 0.069$). Together, these findings indicate an association of NGAL with unstable plaque characteristics.

Immunohistochemistry demonstrated the expression of NGAL in SMCs, macrophages, and endothelial cells (*Figure 2A–D*). High NGAL expression was mainly observed in macrophages, and although NGAL expression was observed in SMCs and endothelial cells in the carotid plaques, their number was limited. *Figure 2B* shows an example of luminal endothelium with staining absent for NGAL. Additionally, neutrophils were examined as a possible source of NGAL within the plaques; however, none or very few neutrophils could be observed. Therefore, neutrophils are probably not an important source of NGAL in carotid atherosclerotic plaques.

3.4 Release of NGAL from atherosclerotic plaques

In blood, drawn directly from the carotid artery containing the atherosclerotic plaque ($n = 9$), NGAL levels tended to increase when compared with NGAL levels in peripheral blood samples drawn at the same time (*Figure 1D*; $P = 0.06$). A comparison of NGAL/MMP-9 complex levels (ELISA) in the plaque related to peripheral blood samples revealed a statistically significant increase in NGAL/MMP-9 complex level in the plaque-related blood samples (*Figure 1E*, $P = 0.007$).

3.5 Mice/MRI

Positive NGAL staining and signs suggestive for buried fibrous caps [positive SMC staining (α-SMA)] were observed in the brachiocephalic artery of an apoE$^{-/-}$ mouse (see Supplementary material online, *Figure S3B* and *C*, respectively) and in aortic plaques of apoE$^{-/-}$/eNOS$^{-/-}$ mice after an atherogenic diet (see Supplementary material online, *Figure S4A* and *B*, respectively). ApoE$^{-/-}$/eNOS$^{-/-}$ mice showed large atherosclerotic plaques in the abdominal aorta with large lipid cores and many macrophages (*Figure 3A* and *D*).

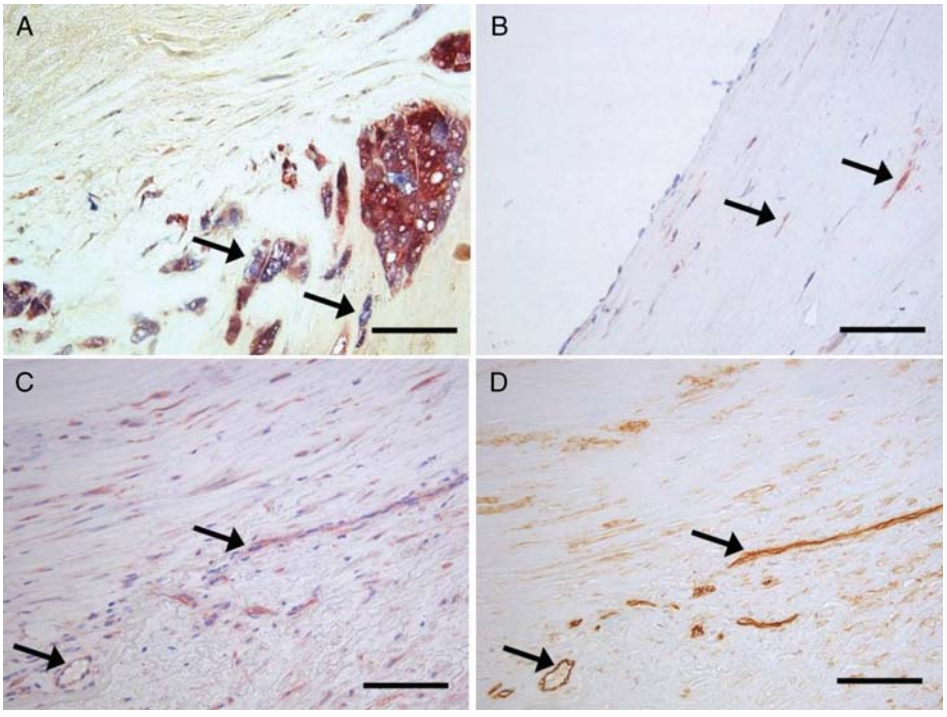

Figure 2 Histology of human atherosclerotic plaques. (*A*) Double staining of NGAL (blue) and macrophages (CD68; red) reveals co-localization (purple). (*B*) NGAL staining observed in SMCs (arrows) but not in inactive endothelium. (*C*) NGAL staining observed in active endothelial cells aligning neovessels, and SMCs. (*D*) CD34+ staining of the same endothelial cells aligning neovessels as in (*C*). Scale bar = 100 μm (original magnification: ×100).

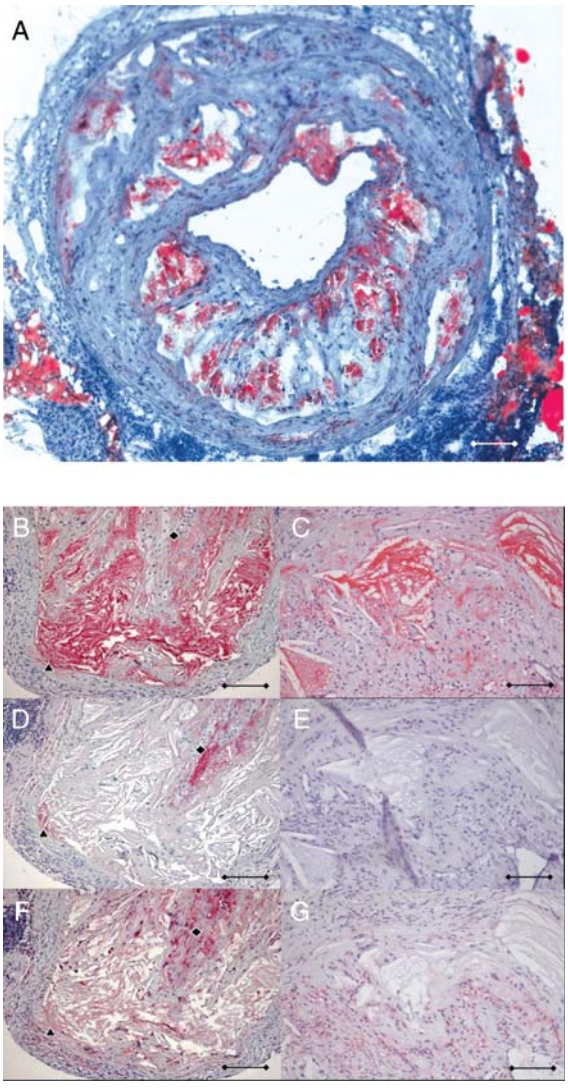

Figure 3 Histology of murine atherosclerotic plaques. Oil red O staining of a representative large aortic plaque with a large lipid core (cryo-section) (*A*). NGAL/24p3 staining (*B* and *C*), micelle staining (*D* and *E*), and macrophage staining (mac-3; *F* and *G*) of aortic plaque in an apoE$^{-/-}$/eNOS$^{-/-}$ mouse injected with NGAL-targeted micelles (*B*, *D*, and *F*) and an apoE$^{-/-}$/eNOS$^{-/-}$ mouse not injected (*C*, *E*, and *G*). Micelles co-localize partially with macrophages (black diamond) and partially with extracellular NGAL/24p3 (black triangle). Scale bar = 100 μm (original magnification: ×100).

MR images showed enhancement at 24 h post-injection both in mice injected with NGAL/24p3-targeted and isotype-conjugated control micelles (*Figure 4*: NER = 1.45 ± 0.14 and 1.31 ± 0.10, respectively). However, at 72 h post-injection, we observed that mice injected with NGAL/24p3-targeted micelles showed more enhancement than mice injected with isotype-conjugated control micelles [*Figure 4*: NER = 1.67 ± 0.12 and 1.21 ± 0.06, respectively ($P < 0.05$)].

Via immunohistochemistry, the specificity of the observed enhancement and detected micelles, macrophages, and NGAL/24p3 was validated. The increase in NER at 72 h in the NGAL/24p3-targeted mice was accompanied by micelle staining which co-localized with NGAL/24p3 expression and the presence of macrophages (*Figure 3B–D*).

As expected, micelles were also found in the glomeruli of the kidneys (data not shown), possibly as a consequence of body clearance.

4. Discussion

MRI shows the most promise for imaging of atherosclerotic plaque vulnerability due to the combined information about anatomic detail and molecular expression. NGAL is a potential novel plaque target for visualization with molecular MRI. The current study reports several new findings regarding the expression of NGAL in human atherosclerotic lesions and its interaction with MMP-9. Moreover, a successful *in vivo* visualization of NGAL/24p3 within murine atherosclerotic plaques was achieved with molecular MRI.

Expression levels of NGAL are associated with unstable plaque characteristics, such as inflammation, and the presence of thrombus or IPH. Previously, these histological characteristics of unstable atherosclerotic plaques have been found to correlate with symptoms in our CEA patients.[33] Both free NGAL and associated with MMP-9 are present in plaques and able to form an NGAL/MMP-9 complex, thereby preserving MMP-9 activity (see Supplementary methods and results).

4.1 The role of NGAL in the plaque

Besides the interaction with MMPs, other functions of NGAL could be important in atherosclerotic plaques. NGAL is implicated to regulate inflammation, because it binds fMLP, leukotriene B4, and platelet-activating factor.[10–12] In addition, NGAL is proposed to be involved in cell survival, but it is disputed if its function is pro- or anti-apoptotic.[34–36] In kidney ischaemia, NGAL protects renal damage by preventing cell death via the induction of haem-oxygenase.[37] Since inflammation, cell death, and ischaemia are key processes in atherosclerosis, free NGAL could play a role in atherosclerotic lesions via these functions but are not addressed in the present study. Here, we focused on the interaction between NGAL and MMP-9 as an important effector mechanism of NGAL in atherosclerotic plaques. In atherosclerotic carotid lesions, NGAL/MMP-9 complex levels were below ELISA detection limits and therefore gelatinolytic activity of the NGAL/MMP-9 complex was measured (see Supplementary methods and results). This demonstrated similar associations with plaque characteristics as free NGAL. The current study is the first to show the coupling of NGAL and MMP-9 in human atherosclerotic plaques, as confirmed by gelatin zymography and western blotting (see Supplementary methods and results), potentially leading to prolonged protease activity (see Supplementary methods and results). The strong association between NGAL plaque levels and MMP-8 activity levels is expected since NGAL was previously shown to be involved in activation of MMP-8.[15]

Features of plaque vulnerability like IPH and buried fibrous caps have been found in plaques of the apoE/eNOS double-knockout mice, similar as can be observed in another animal model of atherosclerosis, the brachiocephalic artery in apoE knockout mice.[30,32] In addition, in both animal models, similar levels of NGAL staining were observed in the brachiocephalic artery.

In order to test whether NGAL deficiency could be associated with reduced incidence of cardiovascular events, we have checked if single-nucleotide polymorphisms (SNPs) are present in NGAL (Affymetrix

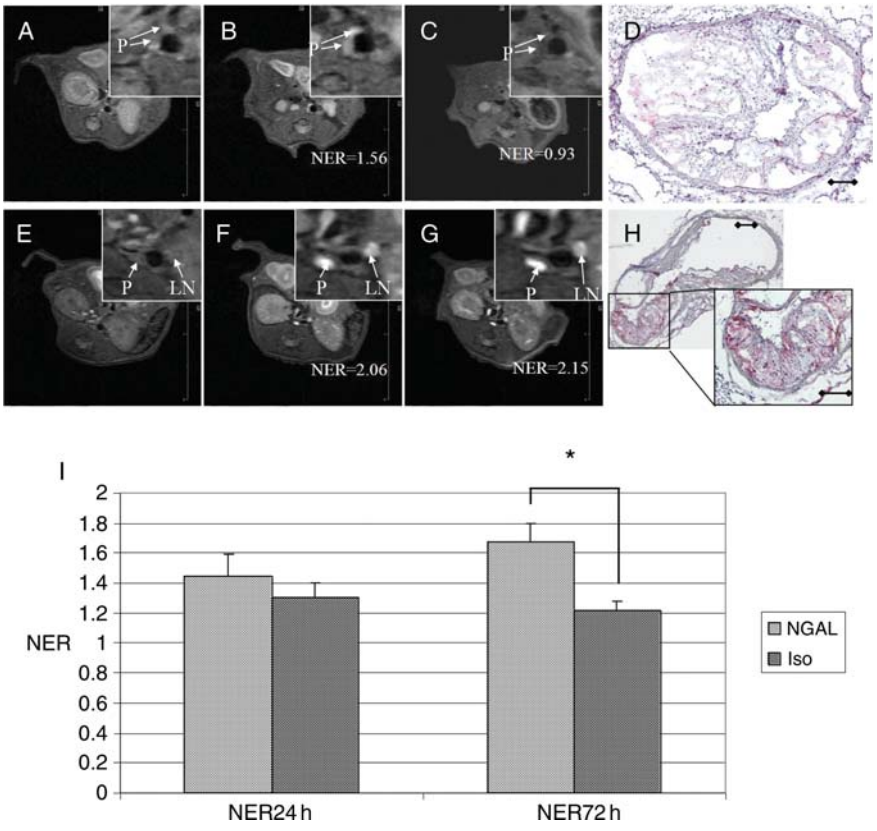

Figure 4 MR images and micelle staining on corresponding levels. Pre- and post-injection (0, 24, and 72 h) MR images of the aortic wall in apoE$^{-/-}$/eNOS$^{-/-}$ mice injected with control (*A*–*C*) and NGAL/24p3-targeted (*E*–*G*) micelles. Histology on murine aorta (72 h after injection) showed no staining of micelles after injection with control micelles (*D*) and extensive red staining after injection of NGAL/24p3-targeted micelles (*H*). P, plaque; LN, lymph node. The post-injection MR images show the enhancement of a lymph node, which was removed during harvesting of the aorta. Scale bar = 100 μm (original magnification: ×100). (*I*) NER at 24 and 72 h after injection of targeted and isotype-conjugated micelles. *$P < 0.05$.

Genome-Wide Human SNP Array 5). Unfortunately, this analysis did not include SNPs, directly or indirectly available, that meet the query criteria (European descent and a linkage disequilibrium, $r^2 > 0.8$). Therefore, we could not assess the relationship between human genetic variation leading to NGAL deficiency and reduced incidence of cardiovascular events within our data set.

A causal link between NGAL deficiency and reduced incidence of athero-thrombosis could be investigated in an apoE/NGAL double-knockout mouse model. Visualization of atherosclerotic plaques in this model using (molecular) MRI would provide the opportunity to find a link between more stable plaques and the lack of NGAL.

The association between NGAL and an unstable plaque phenotype suggested NGAL to be a potential candidate for molecular imaging of high-risk atherosclerotic lesions.

The number of macrophages was not associated with NGAL and NGAL/MMP-9 levels in human atherosclerotic plaques, which is rather unexpected. However, Ronald *et al.*[38] have described the presence of different subpopulations of macrophages (dormant and active) and probably only a part of these active macrophages contribute to the production of NGAL, as we can also observe in the presented staining of macrophages in human atherosclerotic plaque (*Figure 2*). In addition, NGAL (in complex or not) is secreted into the extracellular matrix and stored. This might lead to a relation between unstable plaque phenotypes and increasing levels of NGAL, but without a direct relation with macrophage content.

Some molecular atherosclerotic imaging studies have focused on targets available on macrophage membranes,[39] whereas other studies have targeted ox-LDL, fibrin, or MMPs,[5,40,41] which have extracellular distributions. We may expect that a lot of extracellular targets in atherosclerotic plaque are also present in circulating blood. This could hamper the application of molecular MRI with micelles directed against these targets in patients, because they could bind to the circulating marker before arrival in the plaque. Indeed, in another study regarding the same patient group, the mean NGAL concentration in the plasma was 80 ng/mL, in contrast to the mean plaque NGAL concentration, which was ~120 times higher (unpublished data). We generated Gd-loaded micelles targeting NGAL specifically and observed an increased plaque NER after injection of NGAL/24p3-targeted micelles as compared with isotype-conjugated micelles at 72 h. At 24 h, we could not observe a difference between the two types of micelles, suggesting an early and unspecific uptake of micelles due to the concentration gradient between blood and plaque. However, the level of micelle staining was very diverse among the groups injected with NGAL-targeted micelles. Selection of histological slices and dependency of accumulation of micelles on the degree of plaque neovasculature could be

reasons for this diversity. A non-specific uptake of labelled micelles, probably due to a concentration gradient between the plaque and blood, is seen short after injection (24 h). However, an increased signal between NGAL-targeted and control micelles is present 72 h post-injection.

Although an earlier study revealed a difference in NER at 24 h after injection of targeted vs. non-conjugated micelles, their control micelles lacked an antibody and targeted the macrophage scavenger receptor.[39] Also maximum uptake of micelles targeting oxidation-specific epitopes was reported at 72 h after injection, but isotype-conjugated micelles did not show significant enhancement at any earlier time points.[5] These findings plead for more extended investigation of the MRI timing window for each nanoparticle–target combination.

Generally, fluorescence microscopy is used for *ex vivo* detection of fluorescently labelled paramagnetic micelles. Because of extensive auto-fluorescence of plaque lipids at various emission wavelengths, we used immunohistochemistry on micelle-conjugated rat antibodies. Via immunohistochemistry, we could not observe a difference after injection of targeted and isotype micelles at 24 h; however, the observed enhancement at 72 h post-injection was due to NGAL-targeted micelles since control-targeted micelles could no longer be observed via histology. Micelles of isotype-conjugated and 24p3-targeted micelles were found in glomeruli, suggesting clearance by kidneys. This in contrast to earlier reported predominant clearance of immunomicelles by the liver.[5]

4.2 Conclusions

NGAL is highly expressed in atheromatous human plaques and associated with increased MMP-9 activity. The high plaque to blood ratio of this target in patients and successful visualization of NGAL/24p3 in atherosclerotic plaque of apoE$^{-/-}$/eNOS$^{-/-}$ mice provides a basis for molecular MRI-based risk stratifications.

Supplementary material

Supplementary material is available at *Cardiovascular Research* online.

Acknowledgements

We thank P.H.K., Els Busser, Chaylendra Strijder, Krista den Ouden, K.W.K. and Sander van der Laan for their excellent technical support.

Conflict of interest: none declared.

Funding

This work was supported by the Netherlands Organisation for Scientific Research (NWO) (grant number 016.056.319), the BSIK program (Dutch Program for Tissue Engineering, grant number UGT.6746), and the Netherlands Heart Foundation (grant numbers 2005T102, 2003B249, and 2006T106).

References

1. Stary H, Chandler A, Dinsmore R, Fuster V, Glagov S, Insull W Jr *et al.* A definition of advanced types of atherosclerotic lesions and a histological classification of atherosclerosis. A report from the Committee on Vascular Lesions of the Council on Arteriosclerosis, American Heart Association. *Circulation* 1995;**92**:1355–1374.
2. Briley-Saebo K, Geninatti-Crich S, Cormode D, Barazza A, Mulder W, Chen W *et al.* High-relaxivity gadolinium-modified high-density lipoproteins as magnetic resonance imaging contrast agents. *J Phys Chem B* 2009;**113**:6283–6289.
3. Cormode D, Chandrasekar R, Delshad A, Briley-Saebo K, Calcagno C, Barazza A *et al.* Comparison of synthetic high density lipoprotein (HDL) contrast agents for MR imaging of atherosclerosis. *Bioconjug Chem* 2009;**20**:937–943.
4. Mulder W, Strijkers G, Briley-Saebo K, Frias J, Aguinaldo J, Vucic E *et al.* Molecular imaging of macrophages in atherosclerotic plaques using bimodal PEG-micelles. *Magn Reson Med* 2007;**58**:1164–1170.
5. Briley-Saebo K, Shaw P, Mulder W, Choi S, Vucic E, Aguinaldo J *et al.* Targeted molecular probes for imaging atherosclerotic lesions with magnetic resonance using antibodies that recognize oxidation-specific epitopes. *Circulation* 2008;**117**:3206–3215.
6. Lukyanov A, Torchilin V. Micelles from lipid derivatives of water-soluble polymers as delivery systems for poorly soluble drugs. *Adv Drug Deliv Rev* 2004;**56**:1273–1289.
7. Kjeldsen L, Johnsen A, Sengelov H, Borregaard N. Isolation and primary structure of NGAL, a novel protein associated with human neutrophil gelatinase. *J Biol Chem* 1993;**268**:10425–10432.
8. Triebel S, Blaser J, Reinke H, Tschesche H. A 25 kDa alpha 2-microglobulin-related protein is a component of the 125 kDa form of human gelatinase. *FEBS Lett* 1992;**314**:386–388.
9. Goetz D, Holmes M, Borregaard N, Bluhm M, Raymond K, Strong R. The neutrophil lipocalin NGAL is a bacteriostatic agent that interferes with siderophore-mediated iron acquisition. *Mol Cell* 2002;**10**:1033–1043.
10. Sengelov H, Boulay F, Kjeldsen L, Borregaard N. Subcellular localization and translocation of the receptor for *N*-formylmethionyl-leucyl-phenylalanine in human neutrophils. *Biochem J* 1994;**299**:473–479.
11. Nielsen B, Borregaard N, Bundgaard J, Timshel S, Sehested M, Kjeldsen L. Induction of NGAL synthesis in epithelial cells of human colorectal neoplasia and inflammatory bowel diseases. *Gut* 1996;**38**:414–420.
12. Bratt T, Ohlson S, Borregaard N. Interactions between neutrophil gelatinase-associated lipocalin and natural lipophilic ligands. *Biochim Biophys Acta* 1999;**1472**:262–269.
13. Cowland J, Sorensen O, Sehested M, Borregaard N. Neutrophil gelatinase-associated lipocalin is up-regulated in human epithelial cells by IL-1 beta, but not by TNF-alpha. *J Immunol* 2003;**171**:6630–6639.
14. Yan L, Borregaard N, Kjeldsen L, Moses M. The high molecular weight urinary matrix metalloproteinase (MMP) activity is a complex of gelatinase B/MMP-9 and neutrophil gelatinase-associated lipocalin (NGAL). Modulation of MMP-9 activity by NGAL. *J Biol Chem* 2001;**276**:37258–37265.
15. Tschesche H, Zolzer V, Triebel S, Bartsch S. The human neutrophil lipocalin supports the allosteric activation of matrix metalloproteinases. *Eur J Biochem* 2001;**268**:1918–1928.
16. Galis Z, Khatri J. Matrix metalloproteinases in vascular remodeling and atherogenesis: the good, the bad, and the ugly. *Circ Res* 2002;**90**:251–262.
17. Galis Z, Sukhova G, Lark M, Libby P. Increased expression of matrix metalloproteinases and matrix degrading activity in vulnerable regions of human atherosclerotic plaques. *J Clin Invest* 1994;**94**:2493–2503.
18. Loftus I, Naylor A, Goodall S, Crowther M, Jones L, Bell P *et al.* Increased matrix metalloproteinase-9 activity in unstable carotid plaques. A potential role in acute plaque disruption. *Stroke* 2000;**31**:40–47.
19. Sluijter J, Pulskens W, Schoneveld A, Velema E, Strijder C, Moll F *et al.* Matrix metalloproteinase 2 is associated with stable and matrix metalloproteinases 8 and 9 with vulnerable carotid atherosclerotic lesions: a study in human endarterectomy specimen pointing to a role for different extracellular matrix metalloproteinase inducer glycosylation forms. *Stroke* 2006;**37**:235–239.
20. de Nooijer R, Verkleij C, der Thusen J, Jukema J, van der Wall E, van Berkel T *et al.* Lesional overexpression of matrix metalloproteinase-9 promotes intraplaque hemorrhage in advanced lesions but not at earlier stages of atherogenesis. *Arterioscler Thromb Vasc Biol* 2006;**26**:340–346.
21. Gough P, Gomez I, Wille P, Raines E. Macrophage expression of active MMP-9 induces acute plaque disruption in apoE-deficient mice. *J Clin Invest* 2006;**116**:59–69.
22. Hemdahl A, Gabrielsen A, Zhu C, Eriksson P, Hedin U, Kastrup J *et al.* Expression of neutrophil gelatinase-associated lipocalin in atherosclerosis and myocardial infarction. *Arterioscler Thromb Vasc Biol* 2006;**26**:136–142.
23. Kuhlencordt P, Gyurko R, Han F, Scherrer-Crosbie M, Aretz T, Hajjar R *et al.* Accelerated atherosclerosis, aortic aneurysm formation, and ischemic heart disease in apolipoprotein E/endothelial nitric oxide synthase double-knockout mice. *Circulation* 2001;**104**:448–454.
24. Verhoeven B, Velema E, Schoneveld A, de Vries J, de Bruin P, Seldenrijk C *et al.* Athero-express: differential atherosclerotic plaque expression of mRNA and protein in relation to cardiovascular events and patient characteristics. Rationale and design. *Eur J Epidemiol* 2004;**19**:1127–1133.
25. Beneficial effect of carotid endarterectomy in symptomatic patients with high-grade carotid stenosis. North American Symptomatic Carotid Endarterectomy Trial Collaborators. *N Engl J Med* 1991;**325**:445–453.
26. Endarterectomy for asymptomatic carotid artery stenosis. Executive Committee for the Asymptomatic Carotid Atherosclerosis Study. *JAMA* 1995;**273**:1421–1428.
27. Randomised trial of endarterectomy for recently symptomatic carotid stenosis: final results of the MRC European Carotid Surgery Trial (ECST). *Lancet* 1998;**351**:1379–1387.
28. Halliday A, Mansfield A, Marro J, Peto C, Peto R, Potter J *et al.* Prevention of disabling and fatal strokes by successful carotid endarterectomy in patients without recent neurological symptoms: randomised controlled trial. *Lancet* 2004;**363**:1491–1502.

29. Maier W, Altwegg L, Corti R, Gay S, Hersberger M, Maly F *et al*. Inflammatory markers at the site of ruptured plaque in acute myocardial infarction: locally increased interleukin-6 and serum amyloid A but decreased C-reactive protein. *Circulation* 2005; **111**:1355–1361.
30. Jackson C, Bennett M, Biessen E, Johnson J, Krams R. Assessment of unstable atherosclerosis in mice. *Arterioscler Thromb Vasc Biol* 2007;**27**:714–720.
31. Mulder W, Strijkers G, van Tilborg G, Griffioen A, Nicolay K. Lipid-based nanoparticles for contrast-enhanced MRI and molecular imaging. *NMR Biomed* 2006;**19**: 142–164.
32. Cheng C, Tempel D, van Haperen R, van der Baan A, Grosveld F, Daemen M *et al*. Atherosclerotic lesion size and vulnerability are determined by patterns of fluid shear stress. *Circulation* 2006;**113**:2744–2753.
33. Verhoeven B, Hellings W, Moll F, de Vries J, de Kleijn D, de Bruin P *et al*. Carotid atherosclerotic plaques in patients with transient ischemic attacks and stroke have unstable characteristics compared with plaques in asymptomatic and amaurosis fugax patients. *J Vasc Surg* 2005;**42**:1075–1081.
34. Tong Z, Wu X, Ovcharenko D, Zhu J, Chen C, Kehrer J. Neutrophil gelatinase-associated lipocalin as a survival factor. *Biochem J* 2005;**391**:2–8.
35. Tong Z, Wu X, Kehrer J. Increased expression of the lipocalin 24p3 as an apoptotic mechanism for MK886. *Biochem J* 2003;**372**:1–10.
36. Caramuta S, De Cecco L, Reid J, Zannini L, Gariboldi M, Kjeldsen L *et al*. Regulation of lipocalin-2 gene by the cancer chemopreventive retinoid 4-HPR. *Int J Cancer* 2006; **119**:1599–1606.
37. Mori K, Lee H, Rapoport D, Drexler I, Foster K, Yang J *et al*. Endocytic delivery of lipocalin-siderophore-iron complex rescues the kidney from ischemia–reperfusion injury. *J Clin Invest* 2005;**115**:610–621.
38. Ronald J, Chen J, Chen Y, Hamilton A, Rodriguez E, Reynolds F *et al*. Enzyme-sensitive magnetic resonance imaging targeting myeloperoxidase identifies active inflammation in experimental rabbit atherosclerotic plaques. *Circulation* 2009;**120**: 592–599.
39. Amirbekian V, Lipinski M, Briley-Saebo K, Amirbekian S, Aguinaldo J, Weinreb D *et al*. Detecting and assessing macrophages *in vivo* to evaluate atherosclerosis noninvasively using molecular MRI. *Proc Natl Acad Sci USA* 2007;**104**:961–966.
40. Botnar R, Perez A, Witte S, Wiethoff A, Laredo J, Hamilton J *et al*. In vivo molecular imaging of acute and subacute thrombosis using a fibrin-binding magnetic resonance imaging contrast agent. *Circulation* 2004;**109**:2023–2029.
41. Lancelot E, Amirbekian V, Brigger I, Raynaud J, Ballet S, David C *et al*. Evaluation of matrix metalloproteinases in atherosclerosis using a novel noninvasive imaging approach. *Arterioscler Thromb Vasc Biol* 2008;**28**:425–432.